

## Research Article

# Ground Penetrating Radar: The Electromagnetic Signal Attenuation and Maximum Penetration Depth

**Giovanni Leucci**

*Dipartimento di Scienza dei Materiali, Università del Salento, Via per Monteroni, 73100 Lecce, Italy*

Correspondence should be addressed to Giovanni Leucci, gianni.leucci@unile.it

Received 22 July 2008; Revised 11 November 2008; Accepted 27 November 2008

The use of high frequencies limits the penetration of the radar energy; this low penetration depends, at a parity of used frequencies, on the electromagnetic properties of the investigated material. The principal drawback is the elevated sensibility of the system to the variations of the EM properties of the environment immediately surrounds the antennas. The radar signals that arrive at the receiving antenna are attenuated and modified because of the selective absorption of the pulses by the ground, because of geometrical spreading, and because of an alteration of the actual amplitude due to the instrument amplification. In this paper, the absorption of the radar signal is taken into consideration and we determine, respectively, (i) the radar signal attenuation in the ground, (ii) the electrical conductivity ( $\sigma$ ) and the relative dielectric permittivity (RDP) of the ground, and (iii) the maximum penetration depth of GPR in the ground.

Copyright © 2008 Giovanni Leucci. This is an open access article distributed under the Creative Commons Attribution License, which permits unrestricted use, distribution, and reproduction in any medium, provided the original work is properly cited.

## 1. Introduction

The maximum penetration depth of GPR in the ground is commonly unknown among GPR users because the propagation of the electromagnetic signal depends on the electrical properties of the particular soil at hand. The electrical conductivity of the materials crossed by the EM waves introduces significant absorptive losses, which limits the penetration depth into earth formations and is primarily dependent on the water content and mineralization present. Few studies describe efficient GPR techniques for determining the radar energy attenuation, the relative dielectric permittivity, and the electrical conductivity [1–4]. Several studies, instead, describe efficient laboratory techniques for determining these parameters [5–8].

We present a method to determine the radar energy attenuation directly from the radar sections acquired in the field. The knowledge of the radar energy attenuation is important to identify electrical properties of different materials in the ground (in particular, relative dielectric permittivity (RDP) and electrical conductivity) and to determine the maximum penetration depth of GPR in the ground. To determine the attenuation of the radar, energy has been necessary to find the true value of the radar signal amplitudes. In order to determine the true amplitude of

the radar energy, a technique that allows to remove the gain values from the traces and to correct them for the geometrical spreading has been implemented.

The value of the attenuation of the radar energy has been used to calculate both conductivity and RDP. The value of the electrical conductivity calculated with this method has been compared with the value calculated in laboratory on samples of the same material. The values are in good agreement.

The knowledge of both electrical conductivity and RDP allows calculating the total propagation loss (TPL) [1]. This parameter allows calculating the maximum penetration depth of the GPR in the ground.

In the following, we describe the theory elaborated to determine the radar energy attenuation and demonstrate its effectiveness with an example.

## 2. Background Theory

GPR offers, under favourable conditions, a simple and fast method to provide valuable information on shallow subsurface areas. As said, GPR is an electromagnetic (EM) method similar in principle to the seismic reflection technique, except that it is based on the propagation and reflection of EM waves rather than elastic waves. EM wave propagation is governed by Maxwell's equations, and most

geological media are mainly influenced by the RPD and electrical conductivity ( $\sigma$ ), whereas the influence of the relative magnetic permeability is generally negligible. These parameters affect both wave propagation velocity ( $\nu$ ) and radar energy attenuation ( $\alpha$ ).

$\nu$  and  $\alpha$  are calculated in mks units from the complete theoretical formulas [9]:

$$\alpha = \omega \sqrt{\epsilon \mu} \left\{ \frac{1}{2} \left[ \sqrt{1 + \left( \frac{\sigma}{\omega \epsilon} \right)^2} - 1 \right] \right\}^{1/2}, \quad (1)$$

$$\nu = \frac{1}{\sqrt{(\mu \cdot \epsilon)/2 \left( \sqrt{1 + \sigma^2/(\omega^2 \cdot \epsilon^2)} + 1 \right)^{1/2}}} \quad (2)$$

with  $\mu = \mu_0 = 4\pi \times 10^{-7}$  henry/m,  $\omega = 2\pi f$ ,  $f$  is the frequency in Hz,  $\epsilon = \text{RDP} \cdot \epsilon_0$ , and  $\epsilon_0 = 8.85 \cdot 10^{-12}$  F/m is the dielectric permittivity of the vacuum space.

Abrupt variations of RDP and/or  $\sigma$  cause reflection of the EM energy. Changes in EM properties can often be correlated with changes in the geological structures, facies, and/or internal distribution of properties such as porosity and fluids. The main limitation to cope with is the signal attenuation associated with electrically conductive materials (e.g., clays or ions dissolved in groundwater). Therefore, GPR is well suited for resistive environments. Besides the subsoil properties (but actually related to them), penetration depth also depends on the dominant (central) frequency of the antennas used to transmit the EM energy in the ground and to receive the reflected signal. It is important to outline that the effectiveness of GPR is limited in many problems by its maximum effective range or probing distance (PD) in the medium of interest. This is determined both by radar system limitations and by propagation loss in the material to be probed. The combined effect of the radar system parameters and the absorption parameters of the medium provide the following conventional radar equation (Di Franco and Rubin, 1968) [10]:

$$\begin{aligned} \text{PF} &\geq \text{total propagation loss} \\ &= \text{spreading loss} + \text{absorption loss}, \end{aligned} \quad (3)$$

where PF (in dB) is the “performance figure” defined as

$$\text{PF} = \frac{\text{radiated peak power}}{\text{minimum detectable received signal power}}, \quad (4)$$

where it represents the radar system limitations.

The TPL (in dB) is done by following relationship [1]:

$$\text{TPL} = 10 \log_{10} [8(\text{PD})^3 c/a^4 f(\text{RDP})^{1/2}] + 2(\text{PD})A, \quad (5)$$

where

- (i)  $a$  = antenna aperture;
- (ii)  $c = 3 \times 10^8$  m/s (velocity of electromagnetic waves in vacuum);
- (iii)  $f$  = radar signal frequency;
- (iv) PD = maximum probe depth;

- (v)  $A$  = the absorption loss in decibels per meter =  $8.69\alpha$  dB/m.

For more detailed dealing, the interested reader is addressed to Leucci [3].

### 3. Instrumentation

The instrumentation employed in this work is constituted from the SIR System-2 by Geophysical Survey Systems, Inc. (GSSI, NH, USA).

The tool is a complete digital control with 16 MB of RAM and 450 MB of hard disk.

Its main characteristics are

- (1) input 12 V (DC);
- (2) performance figures (PFs) 160 (dB);
- (3) range from 15 nanoseconds to 2000 nanoseconds;
- (4) frequency of automatic transmission 64 (kHz) (it is the frequency of repetition of the impulse);
- (5) automatic sampling or manual to 128, 256, 512, 1024, or 2048 champions/trace;
- (6) conversion A/D 8 or 16 (bit);
- (7) dynamic range 150 dB.

The types of antennas are

- (a) antenna with central frequency of 35 MHz [monostatic] (Radar Team SUBECHO-40);
- (b) antenna with central frequency of 100 MHz [monostatic] and [bistatic] (GSSI models 3207 with impulse amplitude by 10 nanoseconds);
- (c) antenna with central frequency of 200 MHz (GSSI models 3205 3 nanoseconds);
- (d) antenna with central frequency of 500 MHz [monostatic] (GSSI models 3102A 2 nanoseconds);
- (e) antenna with central frequency of 1000 MHz (GSSI models 3101D 1.1 nanosecond).

### 4. Calculus of the Attenuation

The radar antenna is assimilable, at first approximation, to an oscillating dipole that radiates spherical waves.

The amplitude of the wave that propagates in the ground suffers, therefore, a geometric attenuation (geometrical spreading) due to the distribution of the energy on the front of spherical wave.

At great distances from the source, it is possible to use the approximation of plain wave and, therefore, to use (1) for the attenuation.

One of the goals of this work is to estimate the attenuation directly from the radar traces.

The technique of gain remove constitutes a fundamental point because it is necessary to work with the true amplitude values of the signal and not with the amplified values, usually

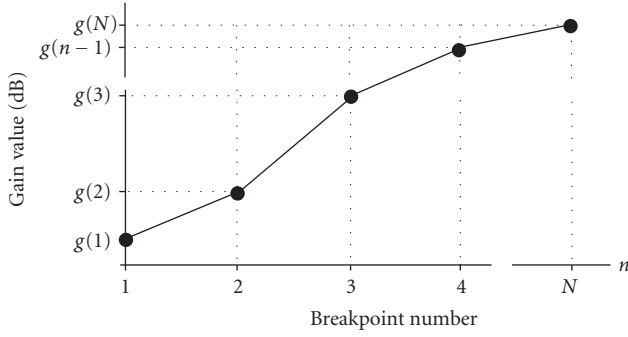


FIGURE 1: Gain function:  $N$  is breakpoint number.

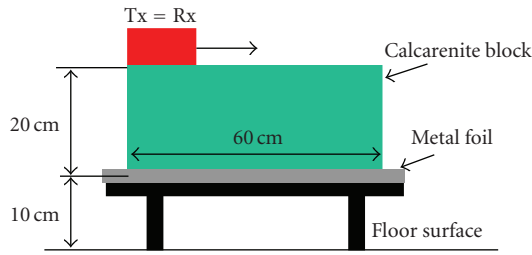


FIGURE 2: Outline of the test performed on the calcarenite block [3].

used in the visualisation of the radar sections. The gain function is (Figure 1) [3]

$$g(n) = g(1) + \frac{g(N) - g(1)}{(N - 1)}(n - 1), \quad (6)$$

where  $n$  ( $n = 1, N$ , and  $N$  is the total samples number) represents the index of the generic sample that varies as far as we move along the axes of the times of the radar section.

In any step, the output amplitude will be

$$A_o(n) = A_i(n) 10^{g(n)/20}. \quad (7)$$

In order to remove the applied gain from the radar traces (7) must be multiplied by  $10^{-g(n)/20}$ .

Before studying the radar energy attenuation, it is, therefore, necessary

- (i) to remove the gain from the radar traces;
- (ii) to correct the amplitude for the geometrical spreading.

The wave amplitude at the time  $t$  is given by

$$A(t) = G(t)A_0 \exp(-\alpha vt), \quad (8)$$

where  $A_0$  is the value of the initial amplitude to the time  $t = 0$ , and the factor of geometrical spreading is  $G(t) = [1/(vt)^2]$ .

The correction for the geometrical spreading is done by multiplying the nonamplified radar traces by  $1/G(t)$ .

Once  $\alpha$  and  $v$  known, one can calculate the average values of  $\epsilon$  and  $\sigma$  by inverting (1) and (2) as follows:

$$\sigma = \left[ \frac{4(\alpha 4 + \alpha 2\omega 2\epsilon\mu)}{(\omega 2\mu 2)} \right]^{1/2}, \quad (9)$$

$$\epsilon = \left[ \frac{(4\omega 2 - \sigma 2v 4\mu 2)}{(4\mu\omega 2v 2)} \right]^{1/2}.$$

At high frequencies and/or very low conductivity, we have [11]

$$\epsilon = \left[ \frac{1}{(\mu v^2)} \right] = \left[ \frac{c}{v} \right]^2. \quad (10)$$

In order to test the validity of these calculations, an experimental test has been performed.

The test was carried out in continuous mode using an antenna with central frequency of 1000 MHz.

Data were collected over a calcarenite block of 20 cm of thickness for 60 cm of length set on two supports to 10 cm of height from the surface of the floor.

To put into evidence, the lower surface of the calcarenite block has been set a metal foil under calcarenite block (Figure 2).

The acquisition parameters are

- (i) time range 8 nanoseconds;
- (ii) samples number 512;
- (iii) gain point 4;
- (iv) gain values [7, 11, 20, 26] dB.

The resulting radar section is shown in Figure 3.

The reflections derived from the upper and lower surface of the calcarenite block are observed in correspondence of 2 nanoseconds and 5 nanoseconds, respectively.

Once it is known, the thickness of the calcarenite block, the electromagnetic wave velocity has been calculated directly using the following relationship:

$$v = \left( \frac{2z}{\Delta t} \right) = 13 \text{ cm/ns}, \quad (11)$$

where  $2z = 40 \text{ cm}$  and  $\Delta t = 3 \text{ nanoseconds}$  (two-way time).

The steps for to determine the radar energy attenuation can be summarised as follows:

- (1) gain remove from the raw radar section;
- (2) correction for the geometrical spreading (using the value of  $v$  previously determinate).

The result has shown in Figure 3(c).

The  $U$  letter in Figure 3(c) points out the value of  $A_0$ . The  $D$  letter in Figure 3(c) points out the value of  $A(t)$  (that represents the lower surface of the calcarenite block).

The value of the radar energy attenuation has been determined as average value of the amplitude in all points of the  $U$  and  $D$  lines (Figure 3(c)).

So, the radar energy attenuation, in the case at hand, is about

$$\alpha = 6.3307 \cdot 10^{-6} \text{ m}^{-1}. \quad (12)$$

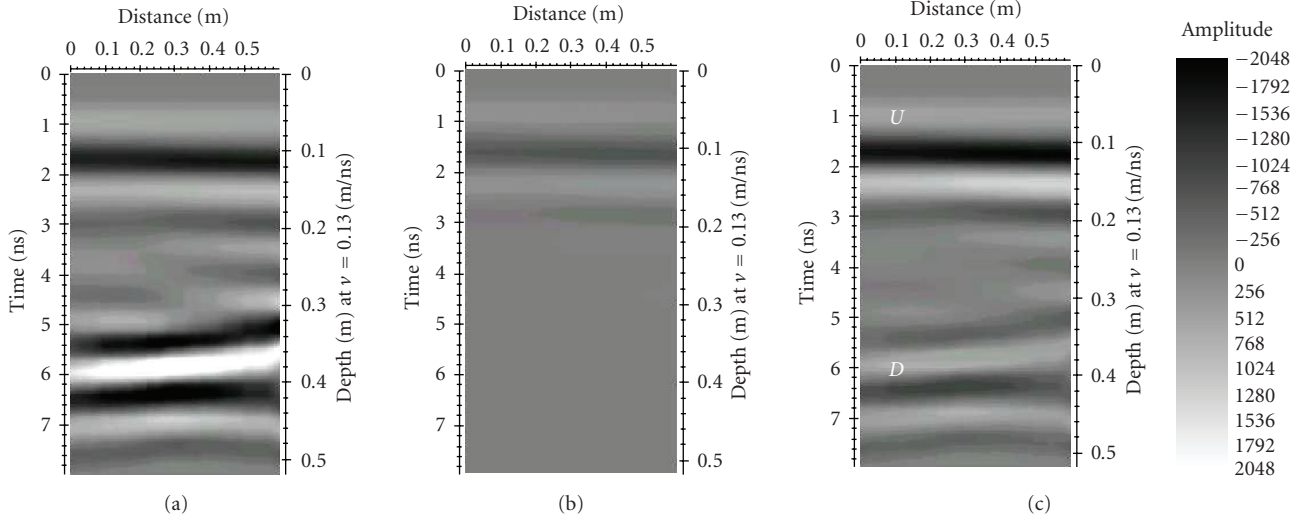


FIGURE 3: Treatment sequence of the data to calculate radar energy attenuation: (a) raw radar section (1000 MHz antenna); (b) remove gain section; (c) section corrected for the geometrical spreading.

From relationships (9) and (10), it is obtained

$$\sigma = 0.224 \cdot 10^{-6} \text{ S/m}, \quad (13)$$

$$(\text{RDP}) = 9. \quad (14)$$

To verify the reliability of the electrical conductivity value (13), we have performed a laboratory test on a sample of the same calcarenite block of dimensions by  $15.3 \text{ mm} \times 13.95 \text{ mm} \times 29.8 \text{ mm}$ .

Using a silver mix, the extremities of the sample have been connected to the voltage generator.

Both the current that passes through the sample and the voltage on its sides were measured .

It has been found that

$$V = 10 \text{ v}, \quad I = 15 \text{ mA}, \quad R = \left( \frac{V}{I} \right) = 0.667 \cdot 10^9 \text{ ohm}, \quad (15)$$

where  $S = 0,213 \cdot 10^{-3} \text{ m}^2$  (calcarenite block section),  $l = 29.8 \cdot 10^{-3} \text{ m}$  (calcarenite block length) from which

$$\rho = R \left( \frac{S}{l} \right) = 4.77 \cdot 10^6 \text{ m ohm} \quad (16)$$

(electrical resistivity of the calcarenite block)

from which

$$\sigma = 0,209 \cdot 10^{-6} \text{ S/m}. \quad (17)$$

This value is in a good agreement with the value of  $\sigma$  worked out from the radar section.

We have, therefore, decided to apply this technique on the data acquired in the field.

A raw radar section relative to a wide-angle refraction reflection (WARR) profile is considered (Figure 4(a)).

The following parameters of acquisition data have been selected for 100 MHz antennas:

- (i) time range 150 nanoseconds;
- (ii) samples number 512;
- (iii) gain [13, 12, 25, 48, 56, 67, 71] dB;
- (iv) the antennas come to move of 0.2 m turned for time.

The wave propagating directly from transmitter to receiver antenna is the ground wave.

In Figure 4(a), several waves are visible. These waves are the direct air wave, the ground wave, and the reflected wave. From all these waves, the ground wave can best be used for wave velocity determination, as its propagation path and the transmitter-receiver spacing are known. We have been estimated a ground wave velocity by 10 cm/ns.

There are some theoretically derived facts about the behaviour of the ground wave. The amplitude of the ground wave decays faster (prop.  $1/r^2$ ), with distance. The amplitude of the ground wave increases in regard to the air wave. On the base of these considerations, we have been determined the radar energy attenuation.

The necessary passages for the radar energy attenuation are shown in Figure 4.

After effecting the operations of ungain (Figure 4(b)) and correcting for the geometrical spreading of the radar signal (Figure 4(c)), we have determined the radar energy attenuation comparing the values of the ground wave amplitude in the red crosses with the value of the air wave amplitude (first cross). In fact, all these points represent the radar energy that has travelled in the ground and that has been received from the receiving antenna.

So, the radar energy attenuation is

$$\alpha = 1.34 \pm 0.09 \text{ m}^{-1}, \quad (18)$$

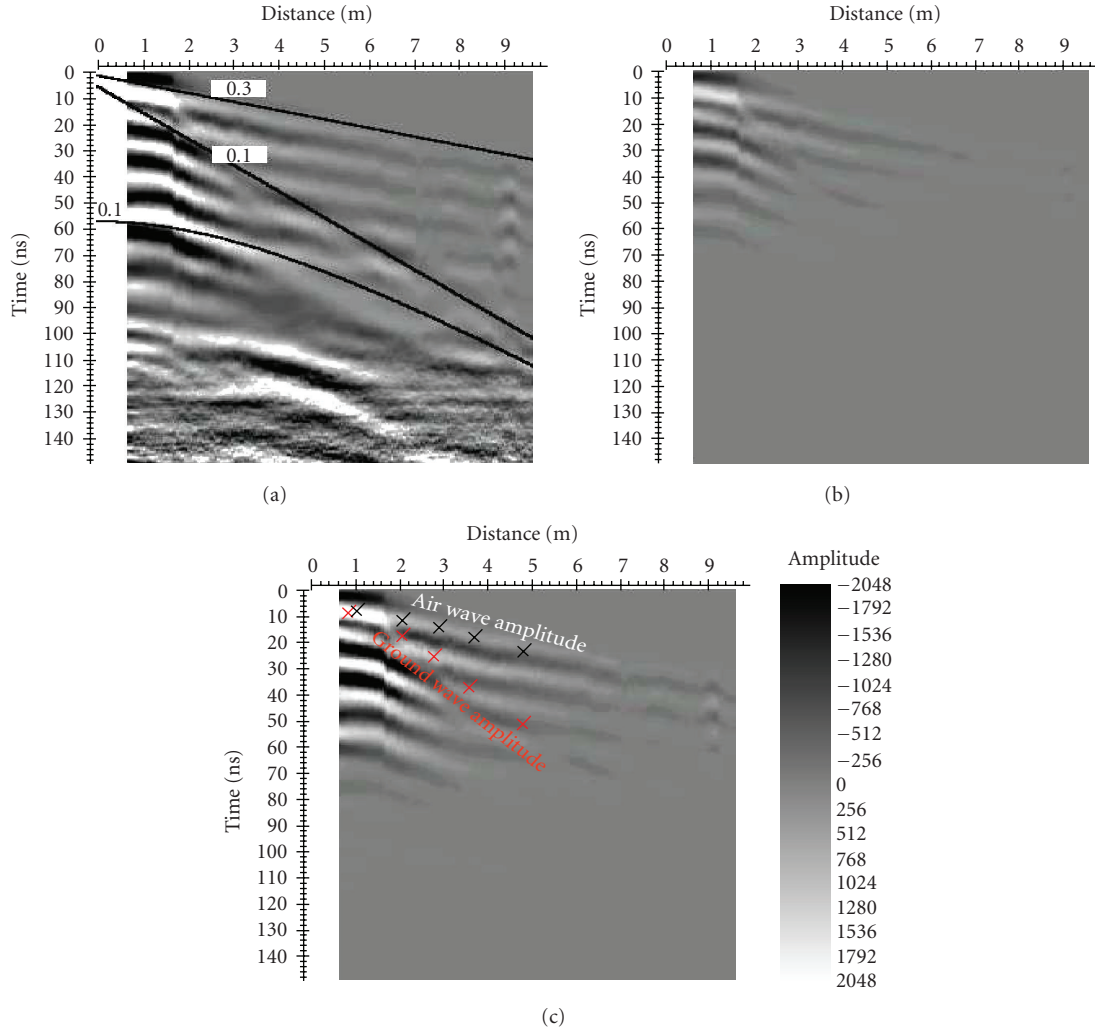


FIGURE 4: Treatment sequence of the WARR data to calculate radar energy attenuation: (a) raw radar section (100 MHz antenna); (b) remove gain section; (c) section corrected for the geometrical spreading.

and the electrical conductivity ( $\sigma$ ), relative dielectric permittivity (RDP), and resistivity ( $\rho$ ) are

$$(RDP) = 4 \pm 0.3, \tag{19}$$

$$\sigma = 0.029 \pm 0.002 \text{ S/m}, \tag{20}$$

$$\rho = \left(\frac{1}{\sigma}\right) = 34 \pm 2.3 \text{ ohm m}. \tag{21}$$

The electrical resistivity value ( $\rho$ ) is in good accord with those found with the geoelectrical survey effected in the same zone.

### 5. Total Propagation Loss and Maximum Penetration Depth

In order to evaluate the GPR maximum penetration depth in the survey area, both the radar energy attenuation and the attenuation due to the instrumentation must be esteemed.

We refer, therefore, to the following relationship

$$PF \geq TPL = 10\log_{10} [8(PD)^3 c/a^4 f(RDP)^{1/2}] + 2(PD)A, \tag{22}$$

In this relationship,

- (i) PF has been furnished by the builder (160 dB in air);
- (ii)  $f$  represents the frequency of centre band of the used antenna (100 MHz);
- (iii) PD is the depth of penetration (unknown);
- (iv)  $a^2$  is the real area of the antenna (unknown);
- (v)  $L$  is the constant of attenuation ( $L = 8.96 \alpha/f$ ) [1].

For the calculus of the TPL, we put in the better conditions  $TPL = PF$  (in air).

In this case, the radar energy attenuation term in the ground in (22) is equal to zero. Unfortunately, in (22), there are two unknown terms PD and  $a^2$ .

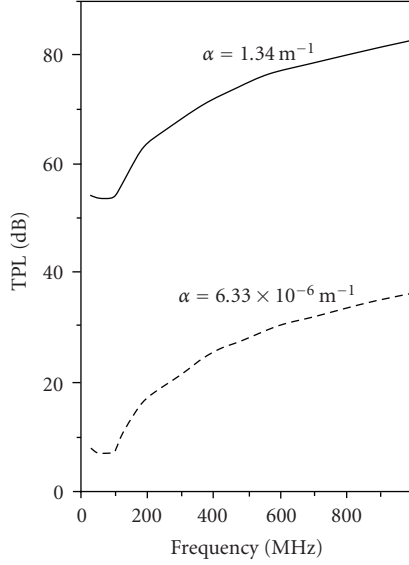


FIGURE 5: Experimental graph of the TPL against antenna frequency.

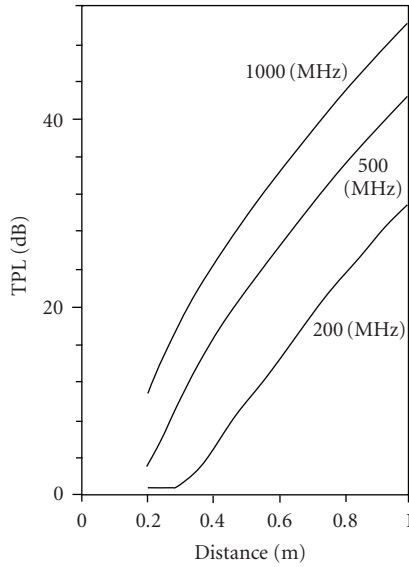


FIGURE 6: Experimental graph of the TPL against penetration depth: the value of attenuation estimated in (18).

For esteem PD, we proceed as follows: we take the relationship that expresses the maximum penetration depth of the radar energy in air:

$$\left[ \frac{2(\text{PD})}{c} \right] = t_{\max}, \quad (23)$$

where  $t_{\max}$  is the maximum time range applicable.

From (18), we have

$$(\text{PD}) = \frac{c t_{\max}}{2}. \quad (24)$$

Once determinate PD, we can calculate  $a^2$  utilising (22).

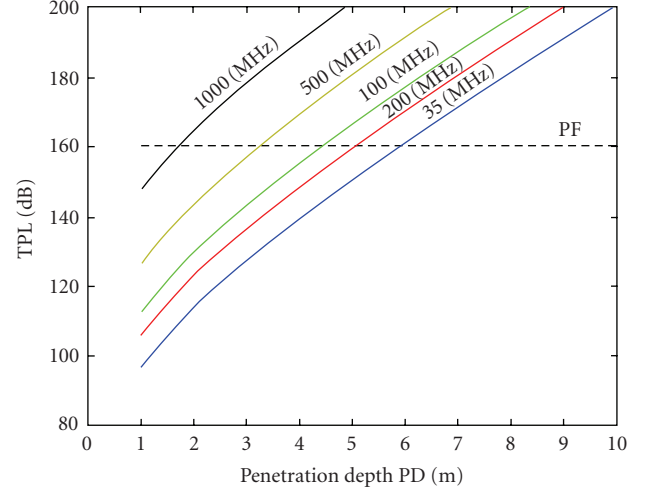


FIGURE 7: Experimental graph of the TPL against penetration depth: the value of attenuation estimated in (18).

TABLE 1: Antenna parameters, determinate in experimental mode, considering the values of attenuation calculated in the field survey.

Antenna frequency (MHz)	Antenna model	Antenna time range (nanosecond)	$a$ (m)	TPL (dB)
1000	HS	20	$2.84 \times 10^{-4}$	82.7
1000	TAD	15	$2.29 \times 10^{-4}$	82.4
1000	TAS	8	$1.43 \times 10^{-4}$	81.7
500	D	100	0.0011	74.8
200	D	300	0.0032	63.1
200	S	150	0.0019	62.1
100	D	500	0.0056	53.8
100	S	250	0.0034	53
35	LF120CM	500	0.0073	54.9
35	LF240CM	1000	0.0123	54

Once esteemed the values of  $a^2$ , that they depend on the antenna, it is possible to esteem TPL in the ground if we have information on the attenuation alfa.

Using the radar energy attenuation value estimated in (18), we have Table 1.

Using both the attenuation values (12) and (18), we get the graph of Figure 5, which represented TPL against antennas frequency. It is important to note that, obviously, TPL decreases with the frequency increase.

Using the attenuation value (18), we get the graph of Figure 6, which represented TPL against depth penetration (PD) in a range of depth (0–1) m for antennas with elevated value of centre band, usually used for investigating small thickness.

A general graph for all antennas used in the field surveys has been represented in Figure 7.

The figures underline the limits (for the penetration depth) associated to both instrumentation and ground.

It is important to note that the maximum depth of penetration is about 6 m (Figure 7) with the antenna by 35 MHz. In fact, the radar sections surveyed in the same site, which has been surveyed the WARR profile of Figure 4, show a strong attenuation of the signal in correspondence of 6 m of depth.

## 6. Conclusions

Since the applications of the GPR depend on the electrical property of the ground, we have focused our attention on the attenuation of the signal and on the EM propagation velocity for having information on the parameters (RDP) and  $\sigma$  that characterised the materials in the ground.

To estimate the attenuation, it is necessary both to remove the gain from all traces and to correct for the geometrical spreading in order to have the true amplitude of the radar signal. The electrical conductivity value of  $\sigma$  of the calcarenite block has been compared with the electrical conductivity value estimated by with independent laboratory tests, on a small sample of the same material. The two values are in good agreement.

The technique to determine the radar energy attenuation has been, subsequently, applied on the radar section acquired in the real site and, also in this case, the comparison between the value of  $\sigma$  estimated from this radar section and that estimated from a geoelectrical survey has given satisfactory results.

In the final part of the paper, we have assembled our attention on the intrinsic characteristics of the instrumentation that contribute to the attenuation of the signal.

The acquaintance of these parameters, together with the attenuation  $\alpha$ , allows calculating the total propagation loss (TPL) for the survey site.

The acquaintance of  $\alpha$  and  $\nu$  has allowed working out the parameters RDP and  $\sigma$ .

The acquaintance of the TPL is important because it allows determining the maximum depth of penetration for each type of antenna and, therefore, to select the more proper antenna to use for the next surveys (in the same zone) according to the purposes of the investigation at hand.

## References

- [1] J. C. Cook, "Radar transparencies of mine and tunnel rocks," *Geophysics*, vol. 40, no. 5, pp. 865–885, 1975.
- [2] A. Godio and T. Guo, "Characterisation of sandy soil with georadar measurements," *Journal of Technical & Environmental Geology*, no. 4, pp. 17–27, 1998.
- [3] G. Leucci, *Prospezioni elettromagnetica e di sismica a riflessione: studio della influenza dei parametri strumentali sul rapporto segnale/rumore*, Tesi di Laurea in Fisica, Dipartimento di Scienza dei Materiali, Università di Lecce, Lecce, Italy, 1999.
- [4] P. M. Reppert, F. D. Morgan, and M. N. Toksöz, "Dielectric constant determination using ground-penetrating radar reflection coefficients," *Journal of Applied Geophysics*, vol. 43, no. 2–4, pp. 189–197, 2000.
- [5] G. C. Topp, J. L. Davis, and A. P. Annan, "Electromagnetic determination of soil water content: measurements in coaxial transmission lines," *Water Resources Research*, vol. 16, no. 3, pp. 574–582, 1980.
- [6] P. N. Sen, C. Scala, and M. H. Cohen, "A self-similar model for sedimentary rocks with application to the dielectric constant of fused glass beads," *Geophysics*, vol. 46, no. 5, pp. 781–795, 1981.
- [7] S. Feng and P. N. Sen, "Geometrical model of conductive and dielectric properties of partially saturated rocks," *Journal of Applied Physics*, vol. 58, no. 8, pp. 3236–3243, 1985.
- [8] G. R. Olhoeft and D. E. Capron, "Laboratory measurements of the radio-frequency electrical and magnetic properties of soils from near Yuma, Arizona," Open-File Report 93-701, USGS, Washington, DC, USA, 1993.
- [9] G. Franceschetti, *Campi Elettromagnetici*, Bollati Boringhieri, Torino, Italy, 1983.
- [10] J. V. DiFranco and W. L. Rubin, *Radar Detection*, Artech House, Dedham, Mass, USA, 1968.
- [11] J. L. Davis and A. P. Annan, "Ground-penetrating radar for high-resolution mapping of soil and rock stratigraphy," *Geophysical Prospecting*, vol. 37, no. 5, pp. 531–551, 2006.